

EMBEDDED SOLID-STATE COOLING LAYER CONFIGURATIONS IN POWER ELECTRONICS

J. Dirker¹, J.D. van Wyk², and J.P. Meyer¹

¹ Department of Mechanical and Aeronautical Engineering, University of Pretoria, South Africa, jaco.dirker@up.ac.za

² Centre for Power Electronic Systems, Virginia Polytechnic Institute and State University, U.S.A.

ABSTRACT

The use of embedded solid-state cooling inserts to increase the power densities in power electronic modules seems promising. Numerical simulations have been used to evaluate the cooling performance of embedded layers into volumes with low thermal conductivity. The impact of thermal interfacial resistance on cooling performance of such schemes was determined. Typical interfacial resistance values were obtained experimentally. Experimental verification of numerically obtained cooling performance increases of cooling layer schemes was done. An increase of 167% in allowed effective heat generation density was achieved in an initial power electronics test case using aluminium nitride to reduce the peak temperatures of ferrite. Functional and thermal optimisation was performed in terms of geometric dimensions. Miniaturisation of cooling layers will improve thermal-magnetic performance only if thermal interfacial resistance values are sufficiently small.

INTRODUCTION

From literature (Avenas *et. al*, 2002; Shidore *et. al*, 2001; Strydom and Van Wyk, 2002) it is clear that thermal issues are major design considerations, which need to be addressed to aid in the development and improvement of a wide range of electronics and allow for further increases in power densities and volume reduction (Zhao and Lu, 2002; Chen and Lin, 2002). Integration of power electronic converters requires the ability to integrate electromagnetic power passives to achieve high overall power densities (Van Wyk *et. al*, 2002).

Although the loss density in power passives is much lower than that found in power semiconductor devices, the corresponding lower thermal conductivities of the ceramics used in these structures lead to thermal limitations. Though heat transfer and cooling performances obtainable via conduction may be orders lower than that exhibited by convective and evaporative schemes, solid state conductive cooling of power passives lends itself to be a possible economical viable cooling technique due to the low thermal conductivities of other materials present in power passives.

A previous study has shown the feasibility of improving the thermal behaviour of such structures by embedding

solid state cooling inserts into it (Dirker and Meyer, 2003). The presence of these inserts can lower operating temperatures dramatically enabling an increase in power density that can be accommodated by the structures. This is achieved by reducing the thermal resistance from inner regions of electronic components, where heat is being generated, to its surface. On the surface, more traditional methods of heat disposal such as heat sinks and fins can be employed to transfer heat to the environment.

Due to the presence of high magnetic flux densities within power passives, cooling inserts consisting of metal are not suitable. The use of metal would result in interference of electro-magnetic operation of the power passive modules and in itself become a heat source due to eddy current generation.

Suitable embedded cooling materials include those with a relatively high thermal conductivity and a low electrical conductivity such as beryllium oxide, aluminium nitride and synthetic polycrystalline diamond with a thermal conductivities in the region of 270 W/mK, 170 W/mK, and 2300 W/mK respectively.

In addition to the constraint placed on material properties, cooling configurations are restricted to orientations running parallel to magnetic field lines as this reduces interference of field lines. From a thermal-geometric and manufacturing point of view, a recent investigation (Dirker *et. al*, 2004), showed that in the geometric size range of interest to power passives, continuous parallel-running cooling layers are the preferred cooling configuration (See Fig. 1), as opposed to a grid of discreet rectangular inserts. The presence of thermal interfacial resistance was however identified as a major barrier to efficient heat transfer.

Depending on the percentage of volume occupied by the cooling inserts, the effective area of regions responsible for carrying magnetic fields, are reduced by the embedding of foreign materials. A reduction in permeability results in higher magnetic field densities, which opposes the thermal advantage gained by the inclusion of the embedded solids. This leads to an opportunity for magnetic flux density optimisation.

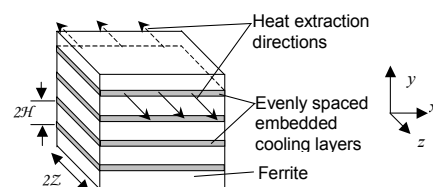


Fig. 1. Preferred embedded cooling configuration for the dimensional range in power electronics.

As an initial step, an embedded parallel-layered cooling configuration was implemented into the outer ferrite layers of integrated electromagnetic power passives. This paper reports on the theoretical analysis of a proposed parallel-layered structure and the optimisation of the increased flux density in the magnetic core material. Experimental validation of theoretical performance increase is discussed.

NUMERICAL ANALYSIS

In order to evaluate and analyse the cooling performance increase due to the inclusion of cooling layers, a numerical model was developed with which the temperature distribution within and around an embedded cooling layer could be determined. As embedded cooling configurations are intended to enhance internal heat transfer within heat-generating components, the success of such a cooling configuration is heavily dependent on the efficient removal method of heat from the surface of the component such as traditional heat sinks and heat spreading plates.

For comparative purposes of different parallel-layered cooling configurations, the surrounding of the heat generating component was defined on two sides as an isothermal body, approximating a heat spreading plate or heat sink, as indicated in Fig. 2. These bodies were not modelled, and their temperature, T_{HS} , was used as a reference point only. In the model heat flow to the environment in the x and y directions were assumed to be significantly less than heat flow in the z direction towards the isothermal bodies. Exposed x - z and y - z faces were defined as adiabatic boundaries. This is valid if the thermal resistances associated with natural convective and radiation heat transfer in the x and y directions are much greater than the thermal interfacial resistance, R_{ext} [m^2K/W] to the isothermal body.

In such a case, the temperature distribution in the x -direction would be uniform and the simulation problem would be reduced to two dimensions. For uniform external interfacial resistance, R_{ext} , identical temperature distributions around and within all cooling layers would exist. In conjunction with the symmetric temperature distribution about the centre of the component, a thermal representative domain was defined as shown in Fig. 2, which can be used to reduce numerical simulation time.

Dimensions \mathcal{B} , b and \mathcal{Z} are defined in Fig. 2 as being respectively half the centre-to-centre distance between cooling layers, half the thickness of a cooling layer and half the z -directional dimensions of the composite structure.

The thermal conductivities of the heat generating material (the electronic component) and the cooling layer are represented by k_M and k_C [W/mK] respectively. In addition to the external thermal interfacial resistance, uniform thermal interface resistances, R_{int} [m^2K/W] was defined on the interface between the heat generating medium and the cooling layer. The volume fraction occupied by the heat extraction layers in terms of the total volume can be expressed by α [-]:

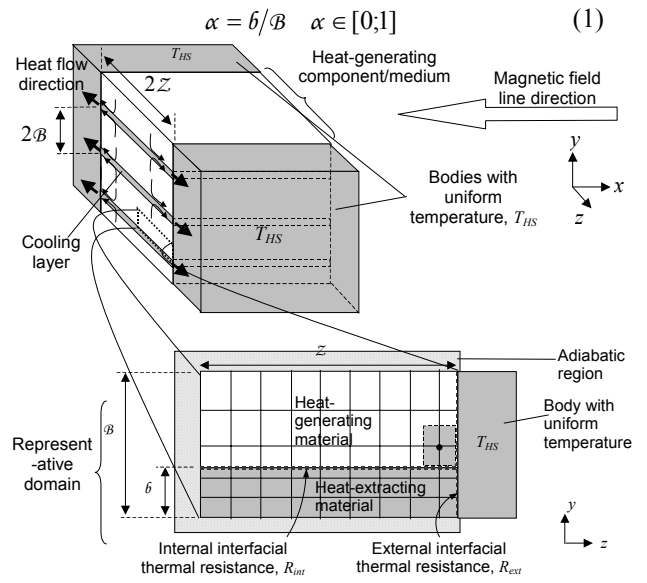


Fig. 2. Two-dimensional model for the analysis of the thermal performance of cooling layer configurations

Steady-state temperature distributions within the representative domain were solved by means of a fully implicit finite difference numerical scheme. A uniform mesh of nodal points was generated in the both the heat generating and the heat extraction regions. The same z -directional spacing was used in both these regions while each region had its own uniform y directional spacing. No nodes were defined on the interfacial surface between the heat-generating medium and the cooling. Mesh densities were chosen such that calculated temperatures varied by less than 1% when the number of nodes in any direction was doubled.

Cooling Performance Calculation

The maximum temperature difference within the domain, ΔT_{max} , found between the peak temperature in the domain and the heat sink temperature can be expressed in terms of the uniform heat generation density, \dot{q}_M [W/m^3] as follows:

$$\Delta T_{max} = \dot{q}_M / C_{GTP} \quad (2)$$

Here C_{GTP} [W/m^3K] is a value depending on the geometric, thermal, and material properties of the domain. With the two-dimensional numerical model this value could be determined for any given set of input values and could then be used as a measure of the cooling performance of the structure. The higher C_{GTP} , the better equipped the structure is to conduct heat to the heat sink.

A case without any cooling layers was defined as the reference for comparative purposes in terms of C_{GTP} . When no cooling layers are present the temperature distribution problem is further reduced to a one-dimensional temperature distribution in the z direction and can be obtained analytically. For such a case, C_{GTP} can be expressed as:

$$C_{GTP,0} = \frac{2k_M}{z^2 + 2k_M R_{ext} z} \quad (3)$$

The performance increase improvement of a cooling layer configuration in terms of the reference case is defined as $E_{\%,eff}$ [%], being the percentage increase in effective volumetric heat generation density that the structure can accommodate while maintaining a given ΔT_{max} :

$$E_{\%,eff} = 100(1 - \alpha) \left(C_{GTM,cooling} / C_{GTP,0} \Big|_{\Delta T_{max}=Const} - 1 \right) \quad (4)$$

IMPACT OF INTERFACIAL RESISTANCE

As heat transfer has to occur over material mismatches, it is necessary to gauge the impact of interfacial thermal resistances at these regions on the cooling performance of the structure. Several numerical case studies were conducted for a wide range of these resistances and their $E_{\%,eff}$ values calculated. For a case where $\beta = 2.5$ mm and $\alpha = 0.1$ with aluminium nitride ($k_C = 170$ W/mK) embedded into ferrite ($k_M = 5$ W/mK), $E_{\%,eff}$ is shown in Fig. 3 for a wide range of internal and external interface resistances. (The chosen dimensional and material property values are of interest to passive power electronics.)

In the idealised case where no interfacial thermal resistances are present, an expected increase of 304% in $E_{\%,eff}$ can be seen. However, as R_{ext} or R_{int} increases, the thermal advantage of inserting cooling layers quickly diminishes. Interfacial resistances are thus a critical factor which influences the effective operation of embedded cooling layers. If these resistances become too great, the advantage of using cooling layers may be nullified. Similar shaped graphs were obtained for a wide range of different input values (Dirker, 2004).

Thermal resistance measurements

Aluminium nitride (AlN), due to its relative low cost in comparison to synthetic diamond was identified as a possible material to be used for cooling layers. Typical thermal conductivity and interfacial resistance values involving “off-the-shelf” aluminium nitride and ferrite was measured using a steady state method.

It was found that the ferrite samples used had a thermal conductivity of close to 5.5 W/mK and the aluminium nitride layers close to 170 W/mK. These results were also independently verified with the aid of a transient laser flash technique. The average surface roughness of the samples was between 3×10^{-7} m to 4×10^{-7} m. All sample surfaces were thoroughly cleaned with acetone before each test was run. Tests were repeated several times.

The processed thermal interfacial resistance values between the ferrite and AlN for a normal pressure range of 100 kPa to 700 kPa on the interface, was found to fall in the region of between 2.2×10^{-4} and 2.5×10^{-4} m²K/W, decreasing as pressure increases. The above-mentioned values were based on data having an experimental scatter of 5%.

Different interfacial mediums including aluminium foil, commercially available thermal pads and high conductivity silver loaded adhesives were also introduced between the AlN and ferrite layers to determine whether the interfacial resistance could be decreased further. It was found that with such materials the interfacial resistances were either very similar or marginally lower.

VALIDATION OF COOLING LAYER PERFORMANCE

In order to validate the numerically obtained cooling performance increase and verify whether embedded cooling can improve thermal conductivity within ferrite cores, an experimental set-up was constructed with which both a reference case, with no cooling layers, and a cooling layer case could be investigated. A schematic representation of the set-up, where cooling layers are present, is given in Fig. 4.

The set-up consisted of a magnetic loop structure operated as the core of an inductor. Depending on the type of test under consideration, the structure could be constructed to either contain alternating AlN and ferrite layers, or just consist of ferrite.

Five layers of ferrite with a height of 4.5 mm and a width of 5 mm were stacked to form a closed magnetic loop. Four rectangular ferrite sections were used to form each level and placed tightly in contact with each other to reduce the influence of the air gaps that might cause uneven magnetic field distribution. AlN slices with a width of 5 mm and a height of 0.5 mm were used as cooling layers when required. In total, 6 AlN layers were used in the ferrite stack when needed.

The test section consisted of one end of the loop and was equipped with 10 calibrated K-type thermocouples with which the temperatures distribution could be monitored. The thermocouples were located both on the surface of the ferrite as well as embedded within the ferrite core as shown in Fig. 4. Heat resistant epoxy and adhesives were used to fix thermocouple locations.

The maximum temperatures could thus be monitored by means of 6 thermocouples, 5 of which were embedded along the z -half-way line of the test section. Temperatures obtained from these thermocouples agreed to within 1°C. Similarly, heat sink temperatures were measured by means of 4 embedded thermocouples (2 thermocouples each), of which readings also agreed within 1°C.

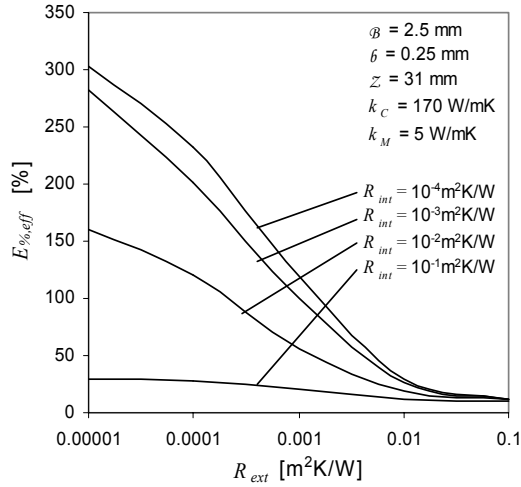


Fig. 3. Effective thermal performance increase

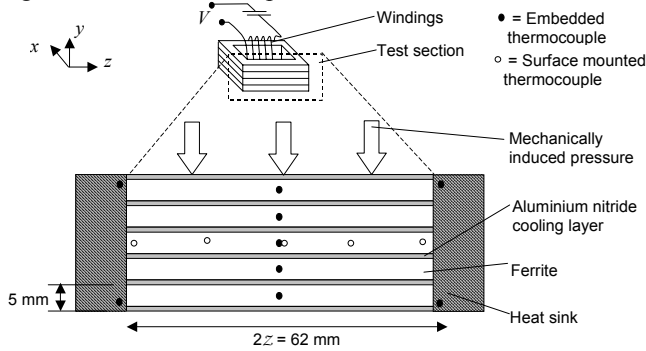


Fig. 4. Schematic representation of validation set-up

For data processing purposes, the maximum test section and heat sink temperatures were taken as the averages of temperatures obtained from each thermocouple group. The wire diameter of each thermocouple was 0.5 mm, which resulted in calculated heat conduction loss via thermocouples to be less than 1% of total heat removal from the test section.

The magnetic material loop structure was held in contact on two sides with identical aluminium heat sinks of. A 12 V DC fan at a fixed position relative to the heat sinks was used to cool the heat sink surfaces. Horizontal clamping was used to maintain pressure between the magnetic loop structure and the heat sinks. Care was taken to apply the same force in all experiments.

In cases where AlN layers were present, good thermal contact was maintained between the AlN and ferrite layers by applying uniform pressure from above. Pre-weighed mass pieces were placed on to the set-up for this purpose. All surfaces except those of the heat sinks were thermally insulated to resemble adiabatic boundaries as closely as possible. The heat transfer between the test section and the other ferrite cores was ignored.

On the opposite end of the magnetic loop, wire was wound around the magnetic core assembly with either 9 or 10 turns. Connecting a capacitor to it in series produced a resonant circuit. Excited with a sinusoidal waveform, the induced magnetic field were assumed to uniformly generate heat within the ferrite core. To effectively heat the ferrite, the operating frequency was set at 1 MHz. By altering the

voltage input to the resonant circuit, different heat generation levels could be investigated.

Different magnetic loop structures with or without AlN layers were tested in order to compare the operating temperatures of these conditions with each other. Tests for a particular condition were performed at least twice; each time the set-up was reconstructed from scratch to determine whether results obtained were repeatable. Once the temperature values stabilized, it was assumed that steady state condition was reached. The current and voltage signals measured by an oscilloscope were captured and saved in both graphical and logged text format. A wide spectrum of inductor voltage was investigated to determine the temperature response at different heat generation levels.

PROCESSING OF DATA

Being able to determine the heat generation density within the ferrite core would have enabled direct comparison between numerical results and experimental data by using Eq. (2). Unfortunately, even though the electric current and voltage waveforms were captured during experimental tests, it was not possible to translate this into core heat generation densities, as only elementary equations for certain geometries describing the power loss in magnetic cores were available.

An alternative validation method was developed where the cooling performance increase, $E_{\%eff}$ was used to validate numerical results. Theoretically, it can be shown that there is a direct relation between the heat-generation density within a configuration shown in Fig. 4, and the steady state temperature of the heat sink, T_{HS} . Mathematically this can be expressed as:

$$T_{HS} = T_{\infty} + \dot{q}_M^m / C_{HS} \quad (5)$$

Here T_{∞} represents the free stream temperature of the air around the heat sink, and C_{HS} [m^3K/W] is a value characterising the heat transfer capacities of the heat sink in terms of internal conduction and convection from its surface. When ambient conditions remain constant, the values of T_{∞} and C_{HS} will be constant also. In such cases, an increase in heat generation density would translate into higher heat sink temperatures.

By incorporating (5) into (2) the following equation relating the maximum temperature rise within the test section to the heat sink temperature can be obtained:

$$T_{max} - T_{HS} = (C_{HS} / C_{GTP}) (T_{HS} - T_{\infty}) \quad (6)$$

If the convective conditions at the heat sink are constant, this relation is linear. Experimentally this was found to be true as is shown in Fig. 5. This enabled the calculation of $E_{\%eff}$ by means of the linear gradients, M [-], obtained experimentally for cases with and without cooling layers:

$$C_{GTP,cooling} / C_{GTP,0} = M_{cooling} / M_{no\ cooling} \quad (7)$$

The average gradient for the case with heat extraction was found to be 3.101, while for the case without cooling the

average gradient is 8.883. This gives a performance enhancement factor of 2.67, which translates into an increase of 167% in the effective heat generation density that could be supported due to the presence of the heat extraction action of the AlN layers. With the thermocouples being calibrated to within 0.1 °C, an uncertainty of $\pm 4\%$ (by value) in the experimentally obtained $E\%$ is expected. (For each gradient M , the uncertainty is $\pm 2\%$)

Depending on the exact material property and thermal interfacial resistance values, the numerical results predict an allowed increase in heat generation for a given ΔT_{\max} to be between 173 and 187% (See Fig. 3 which is valid for the experimental test-set-up). The experimentally obtained $E\%$ value is thus in relative close agreement with the expected value. It was concluded that the numerical model could be used to approximate the thermal performance of cooling layer configurations.

MAGNETIC FLUX OPTIMISATION

Where interfacial thermal resistances are sufficiently low, the embedding of cooling layer materials enables an increase in the heat generation density that could be sustained. In magnetic materials this translates into higher magnetic flux densities.

On the other hand, the inclusion of cooling inserts reduces the cross sectioned area of the active magnetic material. It would be of use to estimate the optimum volume percentage that should be occupied by the cooling layers in order to maximise the effective magnetic field density for a specified peak temperature within the structure. This peak temperature can be expressed as a temperature rise, ΔT_{\max} , above that of the controlled heat sink temperature.

If the magnetic field lines are assumed to be uniform, trends of the core loss, P_v , [W/m³] responsible for heat generation can be approximated by the Steinmetz equation (Li *et. al.*, 2001):

$$P_v = C_1 f^{C_2} B^{C_3} \quad (8)$$

Here f [Hz] represents the operating frequency, B [Wb/m²] represents the magnetic flux density and C_1 through C_3 are constants. Here the use of the Steinmetz equation is only intended for relative comparison purposes and not for the precise determination of either core-loss or magnetic field densities.

By ignoring the magnetic flux through the cooling layers and setting P_v equal to \dot{q}_M , the following expression describing the dependence of the effective magnetic flux density, B_{eff} on the fraction of the volume occupied by cooling, α , can be obtained for a unit depth:

$$B_{\text{eff}} = \left(\frac{\Delta T_{\max}}{C_1 f^{C_2}} \right)^{1/C_3} (1-\alpha) C_{GTP}^{1/C_3} \quad (8)$$

Here it should be noted that C_{GTP} is a function of α as obtained from the numerical model. Since C_1 , C_2 , C_3 , ΔT_{\max} , and the operating frequency f are constants, it

enables optimisation of the magnetic flux density, B_{eff} in terms of α .

The optimum α values for a case where a ferrite section ($k_M = 5$ W/mK and $C_3 = 2.25$) with a depth of 62 mm ($z = 31$ mm) is cooled via AlN cooling layers is given in Fig. 6. The graph indicates the relative influences of B and k_C on the optimum α to be used for cooling.

For a case where both R_{int} and R_{ext} is in the region of 0.0002 m²K/W (as with the experimental set-up), the optimum volume fraction is less than in a case where interfacial resistance is negligible small. In general the optimum α reduced as k_C increased and B reduced (layers thinner and closer to each other).

In Fig. 7 the relative trends of maximised magnetic flux densities associated with the optimum α values of Fig. 6 are shown. It may be seen that for a case where the interfacial resistances are in the range of 0.0002 m²K/W that an increase in k_C has a negligible influence on the maximised

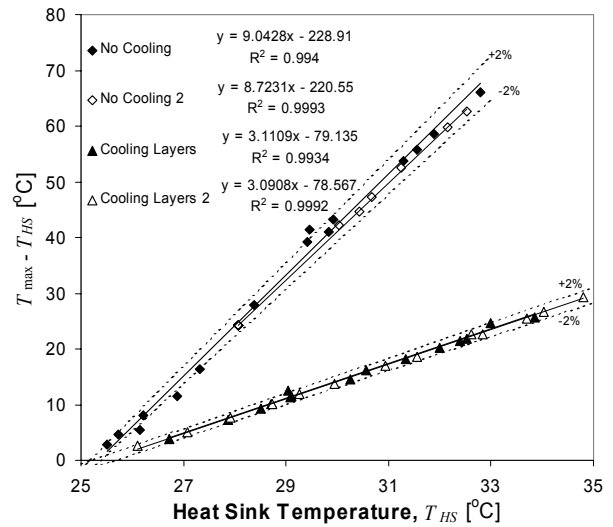


Fig. 5. Experimentally obtained linear relationships

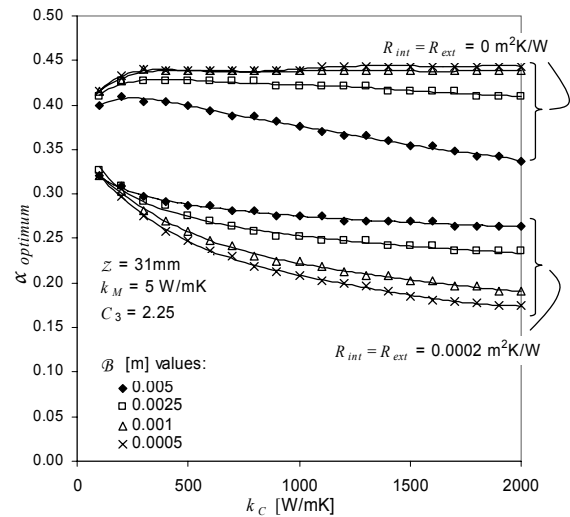


Fig. 6. Optimised magnetic flux density trends.

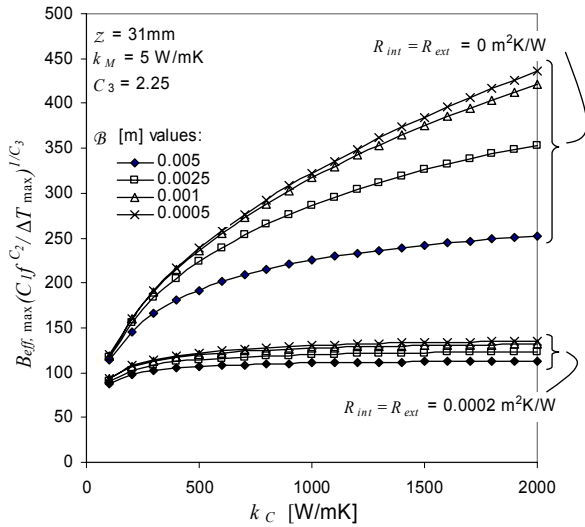


Fig. 7. Optimised magnetic flux density trends. magnetic flux density. A slight increase in the supportable magnetic flux density is expected if β is reduced.

In the case where there is no thermal interfacial resistance it is however expected that both k_c and β would have a significant influence in the maximum magnetic flux density. Similar type trends were found to exist for different values of z .

From these graphs it may be concluded that unless thermal interfacial resistance is reduced to below the levels present in the experimental set-up reported here, little electromagnetic advantage would be obtained by using cooling layer materials with higher thermal conductivities, or cooling layer configuration where the centre-to-centre distance between layers is reduced to within the range of 1 mm.

CONCLUSION

In this experimental investigation it was found that the presence of AlN heat extraction layers decreased the maximum temperature within ferrite operated as the core of an inductor. The experimentally measured effective performance increase of 167% due to the inclusion of cooling layers compared well with the numerical expected performance increase for a test case. Optimum volume fractions occupied by the heat extraction system exist for which in the case of magnetic core material the magnetic field density has a maximum value.

The use of embedded cooling layers to increase the heat generation capacity of passive integrated power electronic modules is promising. However, unless thermal interfacial resistance values are reduced to far below $0.0002 \text{ m}^2\text{K/W}$, little electro-magnetic advantage is expected by using cooling materials with higher thermal conductivities or by using thinner layers in closer proximity to each other.

By reducing the thermal interfacial resistances associated with a cooling layer system, it should be possible to decrease the peak temperatures within the heat generation medium even further, and thus increase the sustainable volumetric power density

NOMENCLATURE

B	magnetic flux density [Wb/m ²]
C_1, C_2, C_3	constants used in the Steinmetz type equation
C_{GTP}	thermal characterisation value [m ³ K/W]
C_{HS}	heat sink characterisation value [m ³ K/W]
$E\%$	allowed volumetric heat generation density [%]
f	frequency [Hz]
k	thermal conductivity [W/mK]
M	gradient of experimental data graph [-]
P_v	magnetic core loss [W/m ³]
\dot{q}_M	volumetric heat generation density [W/m ³]
R	thermal interface resistance [m ² K/W]
T	temperature [K or °C]

Greek and special symbols

α	fraction of volume occupied by cooling [-]
β	half centre-to-centre distance between layers [m]
b	layer thickness [m]
z	half z directional dimension [m]

Subscripts

C	cooling layer
eff	effective
ext	external (towards heat sink)
HS	heat sink
int	between heating medium and cooling layer
M	heat generating medium
max	maximum
0	reference or datum
TS	test section

REFERENCES

- Avenas, Y., Ivanova, M., Popova, N., Schaeffer, C., Schanen, J.-L., and Bricard, A., 2002, Thermal analysis of thermal spreaders used in power electronics cooling, *Conference Record of the 37th I.E.E.E. Industry Applications Conference*, Vol. 1, pp. 216-221
- Chen, P.-C., and Lin, W.-K., 2002, The application of capillary pumped loop for cooling of electronic components, *Computers & Structures*, Vol. 80, No. 1, pp. 23-30
- Dirker, J., and Meyer, J.P., 2003, Optimum rectangular embedded cooling structure shapes in heat generating mediums – A two-dimensional approach. *Proc. 2nd Int. Conference on Heat Transfer, Fluid Mechanics, and Thermodynamics, (HEFAT 2003)*, Livingstone, Zambia, Paper No. DJ1
- Dirker, J., Malan, A.G., and Meyer, J.P., 2004, Numerical modeling and characterization of the thermal behavior of embedded rectangular cooling inserts in modern heat generating mediums, *Proc. 3rd Int. Conference on Heat Transfer, Fluid Mechanics, and Thermodynamics, (HEFAT 2004)*, Cape Town, South Africa, Paper no. DJ1
- Dirker, J., 2004, Ph.D. Dissertation: Heat extraction from solid state electronics by embedded solids with application to integrated power electronic passive modules, *Faculty of Engineering, Rand Afrikaans University, Johannesburg, South Africa*,

Li, J., Abdallah, T., and Sullivan, C.R., 2001, Improved calculation of core loss with nonsinusoidal waveforms, *Proc. 36th I.E.E.E. Industry Applications Conference*, Vol 4, pp 2203-2210

Shidore S., Adams V., and Tien-Yu Tom Lee, 2001, A study of compact thermal model topologies in CFD for a flip chip plastic ball grid array package, *IEEE Trans. Components and Packaging Technologies*, Vol. 24, No. 2, pp.191-198

Strydom, J.T., and Van Wyk, J.D., 2002, Electromagnetic design optimisation of planar integrated passive modules, *Proc. 33rd I.E.E.E. Power Electronics Specialist Conference (PESC), Australia*, Vol. 2, pp. 573-578

Van Wyk J.D., Strydom J.T., Zhao L., and Chen R., 2002, Review of the development of high density integrated technology for electromagnetic power passives, *Proc. 2nd Int. Conference on Integrated Power Systems (CIPS)*, pp. 25-34

Zhao, C.Y., and Lu, T.J., 2002, Analysis of microchannel heat sinks for electronics cooling, *Int. J. Heat and Mass Transfer*, Vol. 45, No. 24, pp. 4857-4869